Materials Selection of Electric Motorcycle Chassis, and Structural Analysis Using Finite Element and Experimental Testing

Freddy Marpaung
Research Centre for Industrial Process and Manufacturing Technology, National Research and Innovation Agency

Arifin
Research Centre for Industrial Process and Manufacturing Technology, National Research and Innovation Agency

Harry Purnama
Research Centre for Industrial Process and Manufacturing Technology, National Research and Innovation Agency

Endra Dwi Purnomo
Research Centre for Industrial Process and Manufacturing Technology, National Research and Innovation Agency

他

https://doi.org/10.5109/7342455

出版情報：Evergreen. 12 (1), pp.303-312, 2025-03. Interdisciplinary Graduate School of Engineering Sciences, Kyushu University, Japan
バージョン：

Materials Selection of Electric Motorcycle Chassis, and Structural Analysis Using Finite Element and Experimental Testing

Freddy Marpaung[1,*], Arifin[1], Harry Purnama[1], Endra Dwi Purnomo[1], Lambert Hotma[1], Wahyu Sulistiyo[2], Eko Agus Nugroho[1], Muizuddin Azka[1], Nasril[1], I Nyoman Artana[1]

[1]Research Centre for Industrial Process and Manufacturing Technology, National Research and Innovation Agency, Gedung Teknologi 2, Kawasan Puspitek, Serpong, South Tangerang, Indonesia

[2]Research Center for Structural Strength of Technology, National Research and Innovation Agency, Gedung BJ Habibie, Jl. M.H. Thamrin No.8, RW.1, Kb. Sirih, Kec. Menteng, Kota Jakarta Pusat, Daerah Khusus Ibukota Jakarta, Indonesia

*Author to whom correspondence should be addressed:
E-mail: fred003@brin.go.id

(Received January 26, 2024; Revised December 19, 2024; Accepted February 1, 2025).

Abstract: A chassis is one of the essential parts of an electric motorcycle, which provides good structural stability to withstand various loading and unloading conditions. The weight and strength of a chassis are important aspects that should be considered during the design stage. The main purpose of this study is to identify the best material for the chassis by combining DLM and FEA. Then, the FEA results are validated by Experimental testing. Different static loading conditions have been applied which is expected to represent various loading condition that occurs in the actual performance of the electric motorcycle frame. In addition, the stress distribution, safety factor, and deformation of the same frame structure with different materials were evaluated to finalize the best suitable material for the chassis on the basis of strength, cost, and weight of the chassis for each loading condition. Based on the DLM method, it has been proposed that an STKM11A is suitable for the analysis compared with other materials in all criteria. The DLM shows that STKM11A is the best material for the platform based on the considered factors. Besides that, the experiment and simulation have a good correlation although some points have the wide gap value such as 14.71% at strain gauge 2.

Keywords: Chassis; Electric motorcycle; Design; Finite element method; Material selection

1. Introduction

A chassis is the main structural component of an automobile. It is the primary supporting structure of an electric motorcycle to which all other frameworks, such as a battery, suspension, and braking and are linked, so the main frame of an electric motorcycle plays an important role to withstand various loading and unloading conditions. During the design stage, it is crucial to consider the weight and strength of the chassis as they determine the characteristics of the vehicle[1,2]. Based on that, It is critical to make the right decisions at this stage to minimize costly consequences later in the development process[3].

The design stage of the electric motorcycle chassis (EMC) structure was initiated by making a 3D CAD model. Based on the 3D CAD model, the strength of the chassis structure was investigated by applying various forces or loads. In order to obtain an appropriate design for the EMC structure, the results of the 3D technical drawing test were then evaluated and updated[4,5]. After the updated prototype is produced, the cycle continues until the final prototype meets safety standards. This conventional process is both time-consuming and expensive[6,7].

This shortcoming can be eliminated by using a virtual model as an alternative to the conventional process of prototype updating and testing[8]. Cali and Oliveri[9], successfully verified the motorcycle frame model by conducting experimental testing. Another work was performed by Rashid et al[10], in which the virtual method was used to design a superbike paddock stand and followed by a virtual test, in which the virtual test results were validated through experimental test data. Scappaticci and co-workers[11] reported the optimization of the chassis model in order to reduce the weight of the vehicle chassis, and without scarifying the stiffness of the frame. Another type of virtual test was conducted by Katdare et al.[12] that used CATIA V5 software to modify and optimize the design in order to reduce the weight of the chassis frame. Patil et al.[13] conducted a finite element analysis study using Ansys on the gearbox component by taking into account load modifications including from the vehicle frame. Gozali et al.[14] had studied a flat carriage chassis simulated using finite element and experimental tests under static and dynamic conditions to determine its strength and durability under operational loading, with the results showing that the stress values were below the fatigue limit curve on the Soderberg diagram. These studies indicated that virtual tests could reduce the time and cost of product development.

Besides the usage of virtual tests in the development of a vehicle chassis frame, materials selection also becomes one of the important aspects that significantly affects the performance and cost[15]. In order to acquire an appropriate material for the EMC structure, we used a digital logic method (DLM) to compare the degree of importance of material properties based on their weighting factors. A study conducted by Fehim and co-workers[16], reported the selection of lightweight materials for close load carriage. Maleeque et al.[17] reported the comparison between DLM and knowledge-based systems for the material selection of automotive pistons. Gustav[18] successfully compared the material selection between the initial DLM and the modified DLM, in which the modified DLM shows superior performance due to better weighting factors. Akinwande et al.[19] successfully conducted material selection from five different materials. They determine some criteria, such as flexural, compressive, and tensile strength, bulk density, thermal conductivity, wear resistance, and water absorption, which are evaluated for the material selection. All studies demonstrated that the use of DLM can improve the performance of the product design. Very recently, Balogun et al.[20] used DLM for material selection to develop eco-friendly and efficient materials for ceiling applications. The best performing material was found to be polypropylene reinforced with 20 wt.% bagasse fiber.

This study introduces an integration of Digital Logic Method (DLM) with Finite Element Analysis (FEA) for material selection and strength analysis, which is a pioneering contribution, as this approach has not been explored in previous research. The stress of the EMC structure was evaluated by conducting a static structural simulation under various loading conditions. To validate the simulation results, a unique experimental method was employed to measure stress on the chassis platform. The primary objective of this simulation was to analyze the stress distribution and deformation of the chassis body across different loading scenarios. This model was investigated at various loading conditions, with a range between 90 and 320 kg. The loading setup refers to the actual loading condition of the chassis. There are some configuration used, such as : 1) the only front passanger; 2) front passanger and rear passanger; 3) front passanger, rear passanger, and load on the footstep.

2. Methods

2.1 Experimental Design

Testing method can be defined as a series of measurements to obtain strain on the motorcycle chassis. The actual static test rig (Fig. 1(a)) and numerical simulation (Fig. 1(b) and Fig. 1(c)) are shown in figure below. The schematic of the static test rig shown in Fig. 2(a). is integrated with some components, such as (1) actuator, (2) support in the front position, (3) support in the back position, (4) frame of the motorcycle, (5) data acquisition, (6) swing arm.

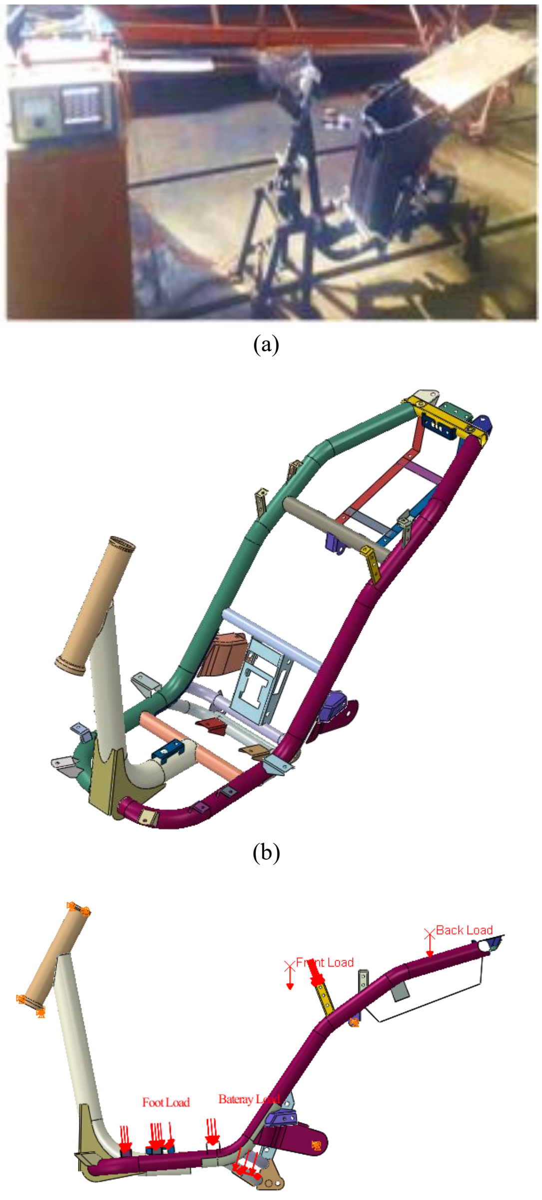

(a)

(b)

(c)

Fig. 1: (a)Static testing scheme for electric motor frames (b)CAD model of the EMC chassis (c)Boundary condition.

Measurement of the strain value is carried out by attaching a strain gauge to the critical point of the electric motorcycle frame according to the calculation results of the finite element method. Strain is defined as the ratio of the increase in length to the original length. A strain gauge consists of a small diameter wire (an etched metal foil) attached to a backing material (usually made of plastic). The wire is looped back and forth several times to create an effectively longer wire. The electrical resistance R of a strain gauge is typically 120 Ω. The strain gauge converts the force applied to the electric motorcycle frame into an electrical signal that can be measured until it is displayed. The force causes strain, which is then measured with a strain gauge by the change in electrical resistance.

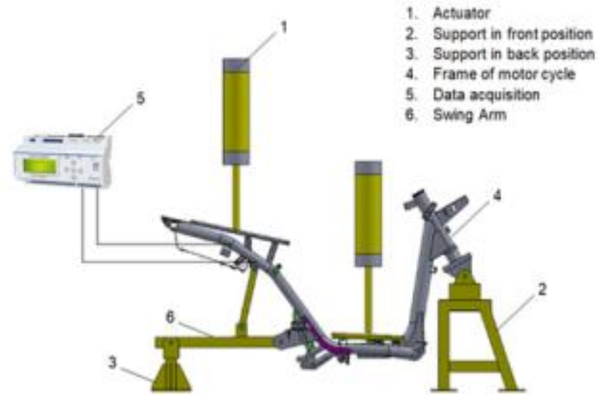

(a)

(b)

(c)

Fig. 2: (a)The static test rig (b)One of the strain gauge locations on the electric motor frame (c)Data acquisition type TDS 530

The strain gauge (Fig. 2 (b)) is mounted on the electric motor frame and connected to data acquisition to display the strain value. Data acquisition works based on the 1/4 Wheatstone bridge theory. One of the resistors is replaced by the strain gauge to measure strain, the type of data acquisition used to measure the strain value on the electric motorcycle frame is TDS 530 (Fig. 2(c)). The data obtained from data acquisition is strain, and then converted into stress value using Hooke's equation, which states $\sigma = E.\varepsilon$, where E = Young's modulus, also called the modulus of elasticity. Young's modulus is assumed to be constant for a given material.

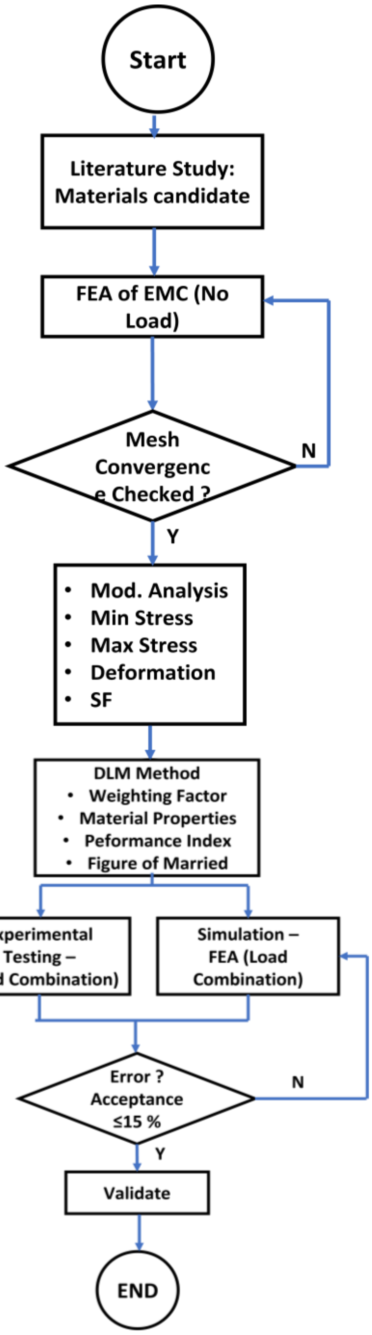

Fig. 3: Flowchart of experiment

The test was carried out to understand the behavior of the EMC structure when applied with various load conditions. This test was carried out with the goal of producing a damaged at chassis components. The test was performed in seven different load series, starting from small value, namely 90 kg, 140 kg, 190 kg, 240 kg, 260 kg, 270 kg, and continued until stress at chassis component approached yield stress (320 kg). Deformation data of chassis components is measured by calculating the values of strain induced at 5 different locations on the EMC structure. Flowchart of the experiment is given in Fig. 3.

2.2 Static Structural Analysis

2.2.1 Numerical Model

Finite Element Analysis was carried out to measure deformation on the electric motorcycle (EMC) chassis. A STKM11A EMC chassis was fabricated upon the completion of the Computer Aided Design (CAD) modeling as well as Finite Element Analysis (FEA). The STKM11A was chosen since it has a better material indexed based on DLM analysis as discussed in Chapter 3.1. The EMC chassis was modeled as beam elements with circular hollow section using CATIA. Then, the CAD model was imported in ABAQUS design modeler. The developed CAD model is shown in Fig. 1(b).

The mathematical formulae used for simulating stress of a static structure are shown in Eq. 1-3.

$$\frac{\partial \sigma_{xx}}{\partial x} + \frac{\partial \sigma_{xy}}{\partial y} + \frac{\partial \sigma_{xz}}{\partial z} + b_x = 0, \quad (1)$$

$$\frac{\partial \sigma_{yx}}{\partial x} + \frac{\partial \sigma_{yy}}{\partial y} + \frac{\partial \sigma_{yz}}{\partial z} + b_y = 0, \quad (2)$$

$$\frac{\partial \sigma_{zx}}{\partial x} + \frac{\partial \sigma_{zy}}{\partial y} + \frac{\partial \sigma_{zz}}{\partial z} + bz = 0, \quad (3)$$

Deformation of material is determined by applying the displacement-strain relations. The gradient of displacement at three coordinates system, as shown in Eq. 4-5, reveals the rate of change of the displacement at specific point in the material.

$$\varepsilon_{xx} = \frac{\partial u_x}{\partial x}, \varepsilon_{yy} = \frac{\partial uy}{\partial y}, \varepsilon_{zz} = \frac{\partial uz}{\partial z} \quad (4)$$

$$\varepsilon_{xy} = \frac{1}{2}\left[\frac{\partial u_x}{\partial y} + \frac{\partial u_y}{\partial x}\right], \varepsilon_{xz} = \frac{1}{2}\left[\frac{\partial u_x}{\partial z} + \frac{\partial u_z}{\partial x}\right], \varepsilon_{yz} = \frac{1}{2}\left[\frac{\partial u_y}{\partial z} + \frac{\partial u_z}{\partial y}\right] \quad (5)$$

A superposition procedure was utilized to incorporate and generalize the stress components from different loading conditions. The relationship between force and strain caused by that force is given by Hooke's law. To improve the accuracy of this method, stress yielded must be linearly related to load and there will be a small-scale deformation in the given model compared to the whole structure. Therefore, Eq. 6-7 are to be used to describe the multiaxial loading of a homogenous isotropic material.

2.2.2 Boundary Condition

The boundary conditions for the static structural analysis showed in Fig. 1(c). In our study we have successfully applied 7 load conditions for the EMC structure, the combinations of diverse load cases have to be taken in order to find the limit capacity of the EMC structure. So, the chassis behaviour under the various loading conditions can be easily understood. The load of the EMC structure consists of the weight of the battery, footstool, and passengers on both sides, front, and rear, which are 20 kg, 50 kg, 125 kg, and 125 kg, respectively.

2.2.3 Mesh Generation

Meshing is a technique to divide the model into several elements. The initiation of any simulation process involves the creation of a mesh, a crucial step often underestimated. To ensure the validity of the simulation results, it's essential to conduct a mesh convergence test, a commonly neglected practice in computational mechanics, which verifies that the results remain consistent despite alterations in the mesh size[21,22].

Convergence studies have been performed by comparing the size of the mesh to the equivalent stress results at one point on the electric motor platform (Fig. 4 (b)). On the one hand, mesh sensitivity analysis was carried out to determine the appropriate element size so that it can be used to model the static load of the electric motorcycle platform. From the meshing analysis in Fig. 4(a), the number of elements generated was 643629, the number of nodes was 650031 and the mesh size of 1.5 mm was chosen for the whole simulation to determine critical areas on the EMC structure.

(a)

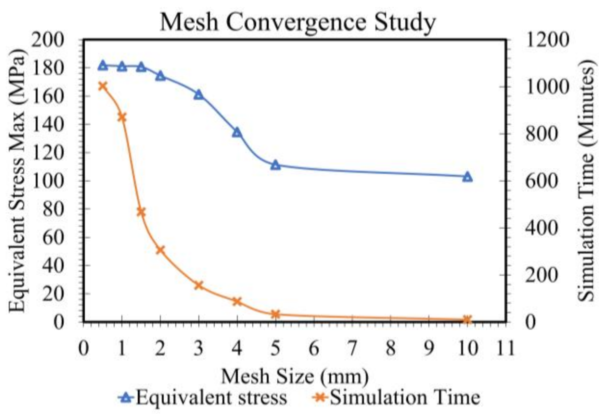

(b)

Fig. 4: (a)Mesh for ABAQUS (b)Mesh convergence

All parts of the electric motorcycle platform are modeled using an S4R element with mesh size between 1.4 mm and 3.6 mm. The element model is a four-node doubly curved linear with reduced integration, which can be used in both thin and thick structural designs[23)]. The advantage of this element model is that the shell element (S4R) can reach a convergent solution faster than other element models[24)]. For all components which used a quad-dominated mesh form with the medial axis algorithm. This medial axis method allows each partition to have at most one singularity by keeping the singularity as far away from the boundary as possible[25)].

2.3 Digital Logic Method

A digital logic method is a material selection procedure that was founded by Morris[26)], and then developed by Farag[27)] by evaluating the material properties by using binary scores to translate their relative importance. This method is divided into three steps:

Firstly, writing the equation for the total number of decisions (N), which is shown in Eq. 9.

$$N = \frac{n(n-1)}{2} \tag{9}$$

where, n is the number of properties of the expected criteria. Secondly, calculating and normalizing the weighting factors to acquire the total value is 1. If a higher property value is desired, then the equation for the scaled properties (B).

$$B = \frac{Numerical\ Value\ of\ property}{Maximum\ value\ of\ the\ list} \times 100 \tag{10}$$

Finally, determine the material performance index (Y), the number of scaled properties is multiplied by the value of the weighting factor. Where, i is the sum of all n relevant properties. The equation can be written as follows.

$$Y = \sum_{i=1}^{n} Y_i \alpha_i \tag{11}$$

The Fig of Merit (FOM) finally determined by using this equation.

$$FOM = \frac{Peformance\ Index}{Cost\ of\ unit\ strength \times 100} \tag{12}$$

3. Results and Discussion

3.1 Material Selection

To investigate the most appropriate materials for the EMC structure, we performed static structural analysis using ABAQUS to obtain some parameters, such as stresses, Factor of Safety (FOS), and deformation. Table 1 showed the comparison of the virtual analysis results for different materials in the EMC structure. Based on the simulation results, it can be seen that material AL 6063-T6 has the lowest value in the three aspects (minimum stress, maximum stress, and safety factor). Interestingly, this material shows good performance on the other parameters, such as deformation.

Table 1. Static structural analysis results (Stress, deformation, safety factor).

Materials	Min Stress	Max Stress	Max Deformation	Safety factor (Min)
STKM11A	7.26E-14	264.9	2.11	1.208
AL 6063-T6	2.53E-13	257.8	6.05	0.931
AISI 1030	2.05E-13	263.7	2.15	1.991
AISI 4130	1.78E-13	265	2.01	2.528

On the other hand, all three other materials showed relatively similar values for each parameter, this is because the three materials have similar properties. To further investigate the properties of each material, we conducted a modal analysis to measure the natural frequencies of the EMC structure by using ten (10) vibration modes for a specific range of frequencies (0 to 300 Hz).

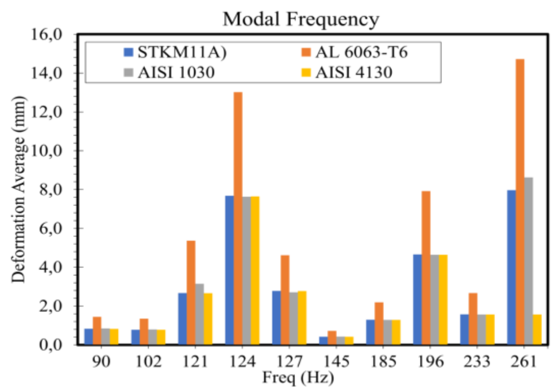

Fig. 5: Modal frequencies of the EMC structure for different materials.

Figure 5 shows that material AL 6063-T6 has a higher deformation rate compared to others in the frequency range between 100 to 150 Hz. Interestingly, all other three materials showed relatively similar deformation values between the specific range of frequency, in particular, STKM11 A has the lowest deformation rate compared to others. Based on the static simulation and modal analysis results, DLM analysis is performed in order to acquire the most suitable material to be used for the EMC structure. The DLM analysis is initiated to determine the weighting factor, which is developed from five different criteria in the form of binary numbers to show a positive decision. The weighting factor is normalized to 1 prior to its value determined. Based on Table 2, the weighting factor for the strength and cost was higher than among other parameters.

Table 2. Comparison of pairwise in weighting factor.

Goals	Number of Decision 1	2	3	4	5	6	7	8	9	10	Positive decisions	Weighting factor
Yields Strength	1	0	1	1							3	0.3
Density	0				1	1	0				2	0.2
Weld-ability		1			0			0	0		1	0.1
Corrosion Resistance			0			0		1		0	1	0.1
Cost				0			1		1	1	3	0.3

This means that strength and cost are important aspects that will be considered for further analysis. Table 3 shows the material properties and cost for four (4) different materials. These properties will be used for the calculation of the performance index (Eq. 11). However, these material properties values have to be normalized using Eq. 10 prior to determining the performance indexed (Table 4).

Table 3. Material properties and cost for various materials.

No	Materials	Yield Strength (MPa)	Density (kg/m3)	Weldability Scale	Corrosion Resistance Scale	Cost ($/kg)
1	STKM11A	290	7800	3	3	0,7
2	Al 6063-T6	215	2700	5	5	2,5
3	AISI 1030	440	7850	4	3	0,78
4	AISI 4130	435	7850	4	3	0,65

Based on previous works, the performance index is sufficient to be used as an indicator for scoring the level of importance of the parameters. However, in this study, we elaborate more detailed material about strength and cost by calculating their FOM using (Eq. 12) and ranking their values as shown in Table 5.

Table 4. The normalization of the performance index.

No	Materials candidate	1	2	3	4	5	Performance Index (Υ)
1	STKM11A	65.9	34.62	60	60	92.86	66.55
2	AL 6063-T6	48.9	100	100	100	26	62.46
3	AISI 1030	100	34.39	80	60	83.33	75.88
4	AISI 4130	98.9	34.39	80	60	100	72.54

Table 5 clearly showed that STKM11A has a higher FOM value (16.62) which was calculated using Eq. 12. This indicated that all parameters (yield strength, density, weldability, corrosion resistance, and cost) will be a good combination in the material selection process. Based on the DLM, the most suitable material for the EMC structure is STKM11A. Such optimization is needed in the industry in order to obtain maximum profit and good material performance.

Table 5. Material ranking for the EMC.

No	Materials candidate	Relative Cost	Cost of Unit Strength X 100	Performance Index	Figure of Merit	Rank
1	STKM11A	1.08	4	66.55	16.62	1
2	AL 6063-T6	3.85	30.63	62.46	2.04	4
3	AISI 1030	1.2	6.73	75.88	11.28	3
4	AISI 4130	1	5.54	72.54	13.09	2

3.2 Simulation Validation

Simulated result of the material stress was derived from ABAQUS. This simulated result was compared with measured data obtained from the EMC. Stress was measured at 5 different locations. The correlation between simulated and measured data was plotted in Fig. 9(b). Figure 9(b) shows that simulation of the STKM11A chassis to find stress is very close to measured data. Coefficient of determination (R^2) of the simulated and measured stress was 0.998.

3.3 Static Structural and Experimental Testing

Static structural analysis was conducted to determine the stresses and deformation of the EMC structure. This stress analysis allows for identifying high-stress regions and maximum deformation at each component of the EMC structure. Based on the ABAQUS simulation, the maximum deformation of 2.112 mm with a load of 320 kg occurs at the back side of the EMC structure. This happens due to this part of the chassis is the farthest point from a fixed point, which lies at the stern tube. This phenomenon is illustrated as a cantilever beam and hence the maximum displacement arises at the endpoint.

Figure 6(b) clearly showed that maximum stress (179,76 MPa) using Abaqus occurs in the middle upper frame or at the seat stay area. While from the experimental test, the maximum stress is 186.4 MPa. The high-stress region occurs in this part due to the increase of load from the passengers. The maximum stress of 179,62 MPa is below the yield strength of the motorcycle frame material which is 325 MPa. As for the other area of the EMC structure, low stresses were acquired. Thus, the EMC structure and joints are adequately strong to withstand the loading applied to it.

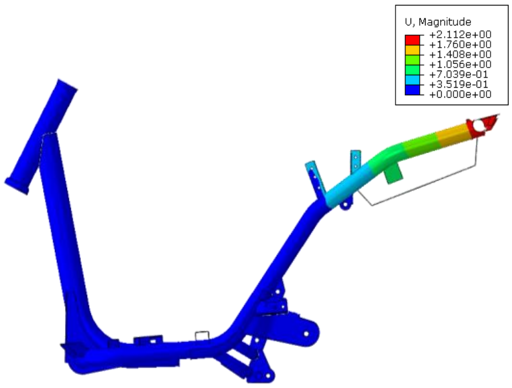

(a)

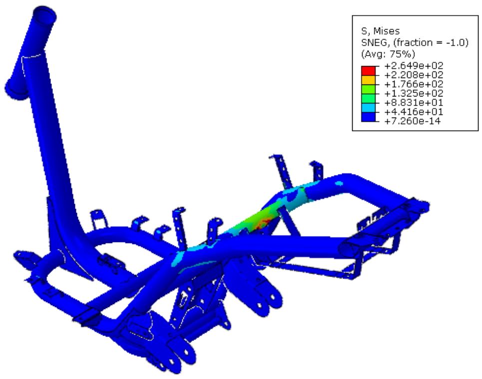

(b)

Fig. 6: (a)Maximum deformation (b)Von-misses stress with a load of 320 kg

In order to acquire the value of the rate of deformation on various load conditions in a structure, the use of a strain gauge is essential because of its ability to measure a change of electric resistance due to the deformation of a structure at a specific load, as shown in Fig. 6(a). In this study, an experimental test is performed to validate the ABAQUS simulation results values.

Stress variation for strain gauges 1,2,3,4, and 5 under a multiplicity of load category is illustrated in Fig. 7-9, in which the maximum percentage of different ratios from the comparative study between experimental test results and ABAQUS results is 14.71% at strain gauge number 2, which is located on the bottom frame, as shown in Fig. 7(b). This phenomenon happens probably because there could be inconsistencies of material surface roughness during strain gauge installation on the EMC structure, which may contribute to the error result between FEA and experimental test. However, because when viewed in other results at other strain gauge positions, the results shows the satisfying result. Besides that, Durgam et. Al[28] and Chinnaraj et. Al[29] reported the similar works which show a good agreement although the error between numerical and experimental analysis is still between 10-15%. Therefore, this simulation result is still acceptable.

As Figure 7(a) shows, the stress values of gauge number 1 increased with the increase of the loading capacity, the same trend is also displayed in the ABAQUS results. From Figure 6, the maximum stress for the experimental test is 13.6 MPa. However, there is still a stress difference between ABAQUS results and experimental results of about 13.97% at 190 kg load capacity. This error might be caused by the effect of roll jig support that makes a negative strain gauge value.

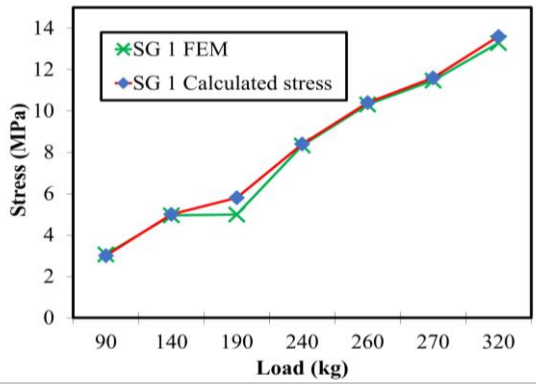

(a)

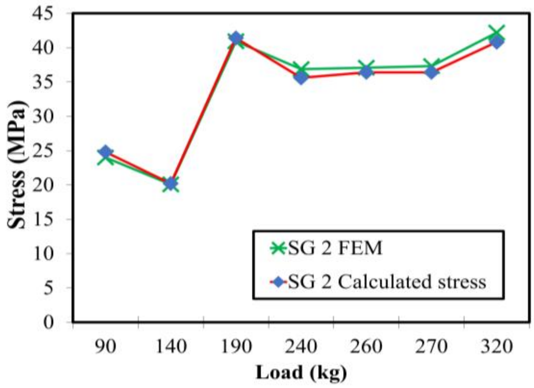

(b)

Fig. 7: (a)Stress vs. load curves from the experimental results and finite element analysis results of strain gauge 1 (b)Strain gauge 2

Also, from Figure 8, it could be observed that experimental stress and simulation stress variation have the same tendency. It was quite clear that simulation stress was slightly higher than the experimental stress. The maximum stress value of strain gauge 2 was up to 40.8 MPa at 320 kg load.

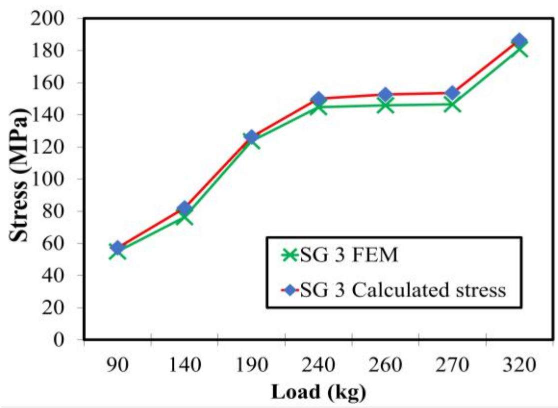

(a)

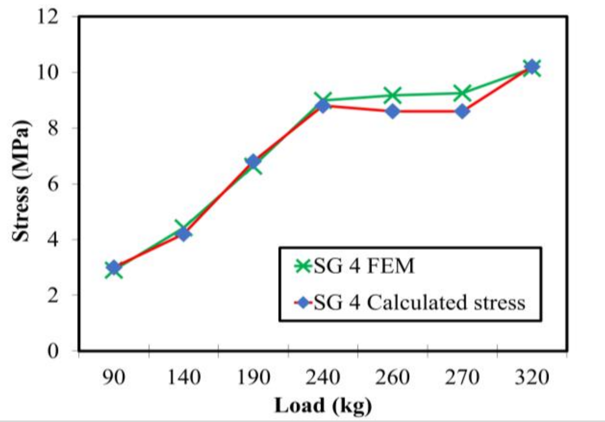

(b)

Fig. 8: (a)Stress vs. load curves from the experimental results and finite element analysis results of strain gauge 3 (b)Strain gauge 4

Figure 9(a) shows the comparison between the two tests in terms of maximum stress values with an increase in the load of the EMC structure. Both test methods have also shown a similar trend of load versus stress. Based on these both results, it shows that simulation test results were the measurement with the least amount of stress at various loads, while the experimental test results have the highest stress values at various loads. The maximum stress value obtained is 186.4 MPa at 320 kg load for strain gauge 5, while the maximum stress from the ABAQUS is 15.89 MPa at 320 kg load. The value of error from Fig. 8(a) was found to be 3%. It shows that ABAQUS results agree well with the experimental test.

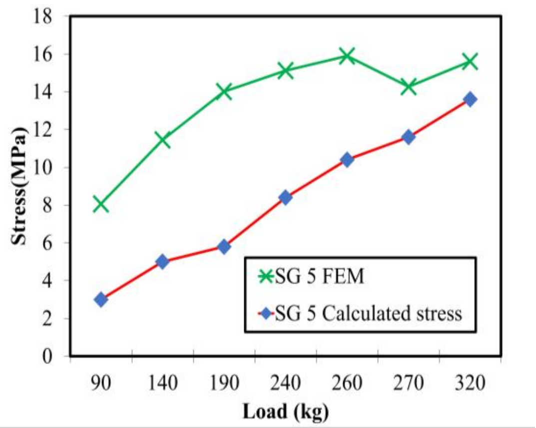

(a)

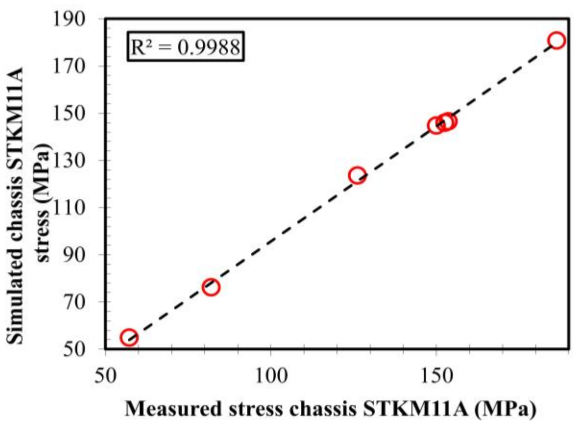

(b)

Fig. 9: (a)Stress vs. load curves from the experimental results and finite element analysis results of strain gauge 5 (b)Validation of simulated stress of STKM11A chassis with measured data

4. Conclusions

The DLM and FEA have been carried out to find the best material and to obtain the Von-Mises stress of the EMC, respectively. Also, the experimental test is conducted to validate the finite element results. DLM showed that STKM11A is the best material for the aspects of strength and cost of the EMC structures. The results showed that the maximum stress for the experimental test is 186,4 MPa was less compared to the simulated result using ABAQUS (180,76 MPa). Simulation results for the STKM11A chassis were found to correlate well with experimental data, indicated from R-squared value 0.998 for stress measurements. It is recommended that in future studies, checks should be conducted on the roll jig support to obtain more accurate values.

Acknowledgements

This work supported by DIPA 2022 from National Research and Innovation Agency Republic Indonesia. The author would also like to thank the technicians of Research Centre for Structural Strength Technology, National Research and Innovation Agency (BRIN).

References

1) P. Jeyapandiarajan, G. Kalaiarassan, J. Joel, R. Shirbhate, F. Felix Telare, and A. Bhagat, “Design and analysis of chassis for an electric motorcycle,” *Mater. Today Proc.*, 5 (5) 13563–13573 (2018). doi:10.1016/j.matpr.2018.02.352.
2) A. Mehra, R. Singh, A.S. Chauhan, K. Nath, and A. Yadav, “Design and analysis of an electric bike chassis,” *Mater. Today Proc.*, 62 1510–1520 (2022). doi:10.1016/J.MATPR.2022.02.247.
3) B. Aerts, M. Deryck, and J. Vennekens, “Knowledge-based decision support for machine component design: a case study,” *Expert Syst. Appl.*, 187 115869

(2022). doi:10.1016/J.ESWA.2021.115869.
4) R.J. Delgado Ojeda, "Motorcycle frame design and optimization," Universitat Politècnica de Catalunya, (2016). http://hdl.handle.net/2117/96944.
5) M. Bagawan, M. Vamsi Krishna, P. Rohit Kumar, K. Gautam Krishna, T. Fatima, and V. Haygriva, "Design and analysis of electric motorcycle chassis frame," *Mater. Today Proc.*, (2023). doi:10.1016/J.MATPR.2023.05.072.
6) M. Hirz, W. Dietrich, A. Gfrerrer, and J. Lang, "Knowledge-based engineering data management," *Integr. Comput. Des. Automot. Dev.*, 393–408 (2013). doi:10.1007/978-3-642-11940-8_8.
7) M. El Alaoui, S. Rabah, V. Chapurlat, V. Richet, and R. Plana, "An original data, information and knowledge management approach for model-based engineering projects," *IFAC-PapersOnLine*, 55 (*10*) 3262–3267 (2022). doi:10.1016/J.IFACOL.2022.10.135.
8) P. MacLeod, "Availability and Capabilities of'low-end'Virtual Modelling (prototyping) Products to Enable Designers and Engineers to Prove Concept Early in the Design Cycle," Prime Faraday Partnership, (2001).
9) M. Calì, and S.M. Oliveri, "Application of an effective simp method with filtering for topology optimization of motorcycle tubular frame," *Int. Rev. Mech. Eng*, 11 (*11*) 836–844 (2017). doi:10.15866/ireme.v11i11.13770.
10) H. Rashid, A.H. Abdullah, M.H.M. Noh, A.H.A. Hamid, and N.M.Z. Abidin, "Design of a superbike paddock stand using cad and cae tools," *Int. J. Automot. Mech. Eng.*, 5 670–679 (2012). doi:10.15282/ijame.5.2012.13.0054.
11) L. Scappaticci, N. Bartolini, E. Guglielmino, and G. Risitano, "Structural optimization of a motorcycle chassis by pattern search algorithm," *Eng. Optim.*, 49 (*8*) 1373–1387 (2017). doi:10.1080/0305215X.2016.1256393.
12) P. Katdare, and S.C. Shilwant, "Design optimization of two wheeler (bike) chassis," *Int. Eng. Res. J.*, 2 4273–4277 (2015).
13) L.N. Patil, A.A. Patil, K.B. Waghulde, S.A. Patil, Y.M. Patil, S.L. Gadhave, V.K. Javanjal, and S.S. Jadhav, "Finite element analysis for improved all-terrain vehicle component design," *Evergreen*, 10 (*3*) 1508–1521 (2023). doi:10.5109/7151699.
14) M. Gozali, M. Nuramin, D.W. Karmiadji, W. Sulistiyo, and H. Purnomo, "Structural strength analysis of 57-ton capacity flat carriage coal transporter with 2x20 feet container subjected to operation conditions," *Evergreen*, 10 (*3*) 2029–2037 (2023). doi:10.5109/7151770.
15) N. Angie, E.M. Tokit, N.A. Rahman, F. Al Zahrah Mohamad Saat, F.S. Anuar, and N.M.M. Mitan, "A preliminary conceptual design approach of food waste composter design," *Evergreen*, 8 (*2*) 397–407 (2021). doi:10.5109/4480721.
16) F. Findik, and K. Turan, "Materials selection for lighter wagon design with a weighted property index method," *Mater. Des.*, 37 470–477 (2012). doi:10.1088/1757-899X/1107/1/012022
17) M.A. Maleque, and A. Arifutzzaman, "Digital logic and knowledge-based system for the automotive piston material selection," *Int. J. Mater. Struct. Integr.*, 6 (*2–4*) 134–150 (2012). doi:10.1088/1757-899X/1107/1/012022
18) G. Jönsson, "Material selection for an aerospace component," (2015).
19) A.A. Akinwande, A.A. Adediran, O.A. Balogun, Y. V Adetula, T.M.A. Olayanju, and O.O. Agboola, "Material Selection for the Production of Roof Tiles using Digital Logic Method," in: IOP Conf. Ser. Mater. Sci. Eng., IOP Publishing, 12022 (2021). doi: 10.1088/1757-899X/1107/1/012022
20) O.A. Balogun, O.O. Daramola, A.A. Adediran, A.A. Akinwande, O.S. Adesina, O.E. Folorunsho, Y. V. Adetula, and O.E. Kolawole, "Development of sustainable polymeric materials for ceiling tiles application and optimization by digital logic method using thermal insulation properties as the functional requirement," *Mater. Today Proc.*, 65 2254–2259 (2022). doi:10.1016/j.matpr.2022.07.092.
21) M.A.P. Perdana, Sudirja, A. Hapid, A. Muharam, S. Kaleg, Amin, R. Ristiana, and A.C. Budiman, "Crashworthiness enhancement: the optimization of vehicle crash box performance by utilizing bionic-albuca spiralis thin-walled structure," *Evergreen*, 10 (*3*) 1961–1967 (2023). doi:10.5109/7151754.
22) E.D. Purnomo, M. Azka, L. Hotma, A. Aziz, K. Herbandono, Nasril, and Arifin, "The prediction of stress and safety factor of shock absorber based on cyclic loading using finite element method," *Evergreen*, 10 (*4*) 2456–2463 (2023). doi:10.5109/7162006.
23) M. Ranjithkumar, and U.P. BT, "Lateral torsional buckling of steel beams strengthened by steel plate," *Mater. Today Proc.*, 49 1670–1673 (2022).
24) B. Schäfer, D. Dörr, and L. Kärger, "Reduced-integrated 8-node hexahedral solid-shell element for the macroscopic forming simulation of continuous fibre-reinforced polymers," *Procedia Manuf.*, 47 134–139 (2020). doi: 10.1016/j.promfg.2020.04.154
25) T.K.H. Tam, and C.G. Armstrong, "2D finite element mesh generation by medial axis subdivision," *Adv. Eng. Softw. Work.*, 13 (*5–6*) 313–324 (1991). doi:10.1016/0961-3552(91)90035-3
26) M.M. Mano, "Digital logic and computer design," Pearson Education India, (2017).
27) M.M. Farag, "Quantitative methods of materials selection," *Mech. Eng. Handbook, Vol. 1 Mater. Eng. Mech.*, 1 531 (2015). doi: 10.1002/0471777447
28) S. Durgam, V. M. Deshmukh, A. P. Jagtap, M. J. Sable, and N. M. Gawai, "Digital logic and

knowledge-based system for the automotive piston material selection," in : IOP Conference Series: Materials Science and Engineering, IOP Publishing, 1126 (2021). doi:10.1504/IJMSI.2012.049952

29) K. Chinnaraj, M. S. Prasad, C. L. Rao, "Experimental Analysis and Quasi-Static Numerical Idealization of Dynamic Stresses on a Heavy Truck Chassis Frame Assembly," *Applied Mechanics and Materials*, 13-14 271-280 (2008). doi:10.4028/www.scientific.net/AMM.13-14.271